

DISSIMILAR WELDING OF DUCTILE CAST IRON TO 304 STAINLESS STEEL

A. M. Sehsah¹, M. M. Ghanem², H. A. Abdel-Aleem³ & M. El-Shennawy⁴

^{1,2,3}Research Scholar, Manufacturing Technology Department, Welding Technology & NDT Lab., Central Metallurgical R&D Institute (CMRDI), Egypt

⁴Research Scholar, Mechanical Engineering Department, Faculty of Engineering, Helwan University, Egypt

ABSTRACT

In this study, effect of welding parameters on microstructure and mechanical properties of dissimilar austenitic AISI304 stainless steel/ductile cast iron DCIA536 joints was investigated. Plates of ductile cast iron (DCI) with 6mm thickness were manufactured, heat treated and inspected at CMRDI casting laboratory. The main welding parameters studied in this work are welding technique (with and without buttering layer at DCI side) and type of filling electrodes. Electrode types applied for this dissimilar joint included Inconel 182 (ENiCrFe-3), cast-iron- Ni-Fe-electrode (ENiFe-CI), and stainless-steel electrodes E309L. Microstructure of welded joints was investigated using optical microscope and scanning electron microscope (SEM) equipped with EDX instrument. Mechanical properties of welded joints were evaluated by hardness test, tensile and Charpy notch impact tests. In general, when using buttering technique at DCI side, it acts as obstacle layer to minimize carbon migration from DCI side to the weld and reduce formation of carbides in weld metal. The sample welded using buttering layer (ER Cu Al-A2) and filling groove with electrode ENiCrFe-3 had better mechanical properties compared with same sample without buttering technique.

KEYWORDS: Dissimilar Welding, Ductile Cast Iron (DCI), AISI 304 Stainless Steel, SMAW, TIG, Microstructure Characteristics, Mechanical Properties

Article History

Received: 25 Apr 2021 | Revised: 27 Apr 2021 | Accepted: 10 May 2021

INTRODUCTION

One of the recent challenges in modern industry is to decrease size designing of components by welding dissimilar materials together. Dissimilar welding of ductile cast iron (DCI) with austenitic stainless steel AIS304 has many applications in different industrial sectors such as oil & refining and petrochemical industries. Strength, corrosion resistance and low-cost maintenance should be considered for dissimilar joints of cast iron to stainless steel in different applications such as welding of cast iron coupling to stainless steel pipes [1].

Welding of DCI / stainless steel AIS 304 has many problems due to poor weldability of cast iron. DCI has higher carbon content compare to stainless steel which diffuses into stainless steel side during welding and forming hard phases such as martensite at heat affected zone (HAZ) of DCI in addition to forming different carbides in weld metal zone (WM) and this leads to crack developing, deterioration of the mechanical properties of weld joints such as poor elongation and high hardness [2]. In addition to previous problems, after welding of DCI/stainless steel, the joint is greatly affected due to degradation of stainless steel due to oxide notch (low corrosion resistance) and other

metallurgical deteriorations at the weld interface and residual stress due to different in thermal expansion. Recently many researchers tried to overcome these problems but all of them still under developing and no technique has been practically applied [3-8]. M. El-Shennawy and A. Omar welded dissimilar joints of cast iron / stainless steel with different welding processes with different techniques. They found that successful welding can be obtained by welding using two different electrodes E6013 and E309 and these techniques lower the hardness and increased the weld metal toughness [9]. E.M. Elbana studied the effect of preheat on weldability of cast iron using welding electrode (ENiFe- CI), it is concluded that DCI can be welded with and without preheat and the mechanical properties of weld joint can be improved by applying high preheat temperature (250~ 300 Co) [10].

E.M. Elbana and et al. again studied restoration properties of welded pearlitic cast iron by Shield Metal Arc Welding (SMAW) process with different welding electrodes with applying post welding heat treatment (PWHT) at 677 °C. They reported that welding by ferritic electrode with 300 °C preheat was the best option to reduce the width of HAZ. They also concluded that PWHT reduce the maximum hardness values of weld metal and HAZ. While using electrodes with high Ni content can reduce carbides formation [11].

Dinesh and et al. reported that dissimilar weld joints of cast iron/stainless steel 304 with different electrodes (ERNiCr-3/ERNiCrFe-3) can be successfully welded using buttering technique (BT). Angular distortion (one measure for residual stresses is reduced and mechanical properties are improved when applying buttering technique due to decrease carbon migration from cast iron side to weld metal and other certain variations in weld metal chemistry which leads to improve the metallurgical properties of weld metal [12].

Because of above mentioned reasons, fusion welding processes of DCI/ stainless steel needs specific requirements and precautions. Other researchers tried to weld this combination with solid state welding in spite of limitation of solid state welding in practical constructions. Sedat Kolukisa has studied the effect of welding temperature on weldability of AISI420 stainless steel / DCI. He concluded that this combination can be joined with diffusion welding process under Argon atmosphere at 800, 900, 1100 °C processes temperature at 20 min, constant time, 12 MPa constant pressure, respectively and the quality of the coalescence at welding interface increased when applied elevated temperature about (1100 °C)[13]. Radoslaw et al. investigated Friction welding of DCI / 321 stainless steel. They found that the process of friction welding was accompanied with diffusion of Cr, Ni and C atoms across the DCI/stainless steel interface. This leads to increase in carbon concentration in stainless steel side where Cr carbides were formed and located at the grain or subgrain boundaries while, the size and distribution of these carbides depended on the distance from weld interface [14].

Shield metal arc welding (SMAW) process considered the most particle welding process for construction as well as for repair welding maintenance. Thus, in this study the authors tried to find the best welding practice technique for welding of DCI/AISI 304 stainless steel joints by SMAW. They studied the effect of different welding parameters such as welding with different and multiple electrodes with and without applying buttering techniques with different filler metals on properties of dissimilar joint of DCI/AISI 304 stainless joint.

EXPERIMENTAL WORK MATERIAL AND WELDING PROCEDURE

Dissimilar welded joints of ductile cast iron (DCI) and stainless steel 304 (AISI304) were welded under various welding conditions using (SMAW) and (GTAW). Welding electrode and welding procedure were the main controlling parameters

applied. Ductile cast iron was produced in a foundry at Casting Technology Department in Central Metallurgical R&D Institute (CMRDI). Machining, finishing and inspection of produced cast plates were carried out by milling and NDT with X-ray, respectively. Chemical composition and mechanical properties of the cast were comparable to ASTM A536 grade [80-55-06]. Table 1 and 2 shows the chemical composition and mechanical properties of DCI and AISI 304 used in this study.

Annealing of DCI base metal improves ductility and elongation, decreases hardness and lowers the probability of finding cracks during welding. Thus, produced DCI was annealed at temperature 900°C with soaking time 1.5 hours. Joint design for all specimens used in this study and the main two techniques followed in this study to weld DCI / 304 stainless steel plates are summarized in Fig. 1 which shows schematically, the welded joints using buttering and without buttering for the dissimilar alloys. Specimens were preheated to 250-300oC and then welded by SMAW & TIG welding processes. Welded specimens were isolated by thermal wool after welding process to avoid rapid cooling in heat affected zone. Welding electrodes used in this study included Inconel 182 (ENiCrFe-3), cast-iron-Ni-Fe-electrode (ENiFe-CI), Al-bronze 90/10 (ER Cu Al-A2) and stainless-steel electrodes E309L. Welding procedures adopted for these dissimilar joints included using single type electrode for filling the V-groove, two types of electrodes one for buttering layer and the other for filling the V-groove. Welding conditions and procedures are detailed in Table. 3.

All welded samples have been examined by non-destructive testing (NDT) such as visual test (VT), dye penetrant test (PT) and radiographic test (RT) to assure quality. All welded specimens were accepted.

The welded samples were prepared for macro and microstructures investigations by grinding and polishing then etched using 2 % Nital reagent for ductile cast iron side of welded joint flowed by electro-etching using oxalic acid for austenitic stainless-steel side of the dissimilar joint. Optical and electron microscope (SEM) equipped with energy dispersive x-ray (EDX) analyzer are used for microstructure examination and phase analysis for welded specimen.

Vickers micro-hardness measurements were carried out at cross sections of welded specimens. Tensile and impact test were carried for welded specimens according to American Society of Mechanical Engineers (ASME) code section IX [15]. As shown in Figures. 2 & 3. Impact test was carried out at room temperature on standard machined specimens taken from predetermined locations in HAZ of DCI and other specimens taken in HAZ of AISI304 welded joints according to ASME code section IX.

Table 1: Chemical Composition of DCI A536 Grade and Stainless Steel AISI 304

Alloy	C	Mn	Si	Cr	Ni	Mo	Cu	P	S	Co	Mg	Fe
DCI (As cast)	3.83	0.28	2.66	0.038	0.27	0.007	0.278	0.022	0.012	0.0024	0.024	Rest
AISI 304	0.055	1.40	0.31	18.8	8.27	-	0.253	0.031	0.001	0.172	-	Rest

Table 2: Mechanical Properties of DCI A536 and Stainless Steel AISI 304

Alloy	Tensile strength, MPa	Yield Strength, Mpa	Elongation, %	Hardness, Hv	Charpy Impact Toughness, J
DCI (annealing)	428	326	19	240	16
AISI 304	644	366	54	129	325

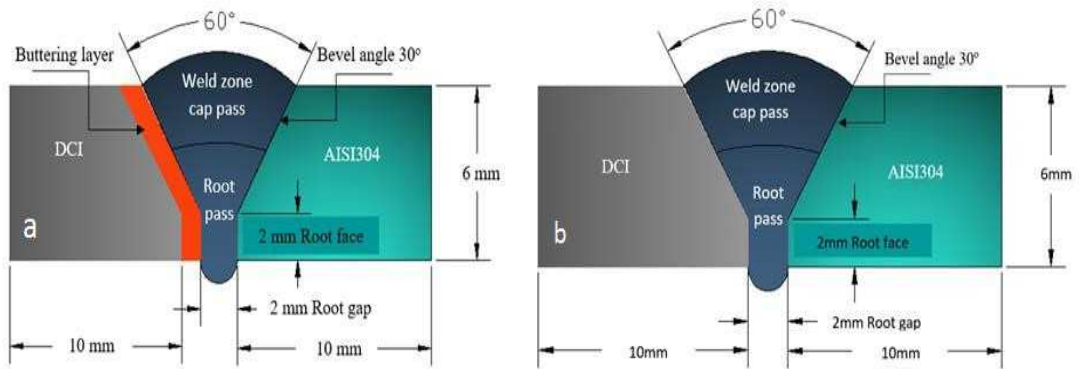


Figure 1: Schematic for Joint Design and Techniques for Welding DCI/AISI304; (A) With Buttering, (B) Without Buttering.

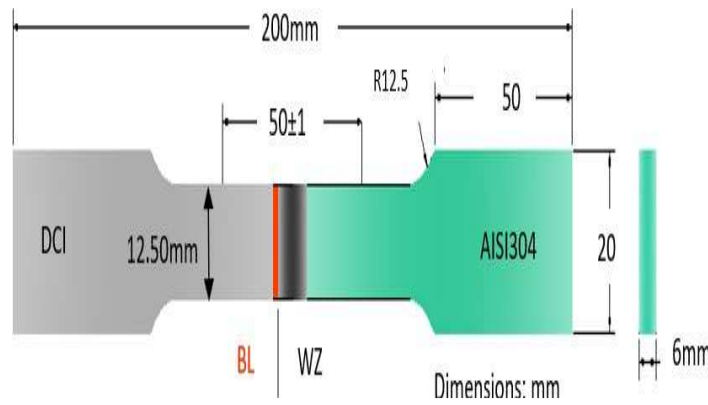


Figure 2: Tensile Test Specimen.

Table 3: Welding Conditions and Procedure

Sample No.	Pass	Electrode	Type of Welding	Electrode Diameter, mm	Ampere	Voltage	Travel Speed, mm/min	H.I, J/mm	
With Buttering	1	1 st	SMAW	3	78	22	109.8	750.16	
		2 nd			80	24	95.2	968.06	
		3 rd			80	28	71.4	1505.88	
	2	1 st	ER Cu Al-A2 Buttering	TIG	3	100	13	76.9	608.58
		2 nd	ENiCrFe-3	SMAW	3	54	21	90.9	598.81
		3 rd				70	24	79.3	1016.89
Without Buttering	1 st	ENiCrFe-3	SMAW	3	63	28	80	1058.4	
	2 nd				80	30	133.3	864.21	

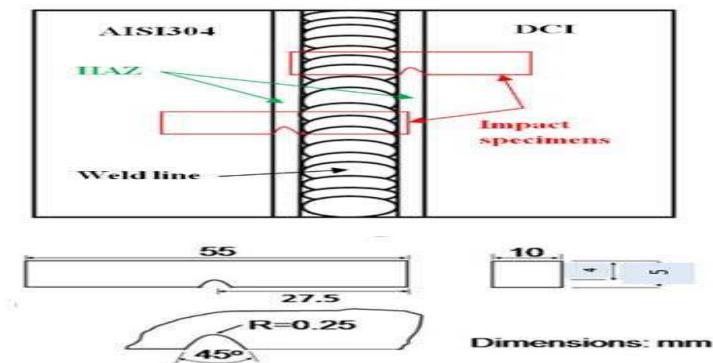


Figure 3: Locations and Dimensions of Impact Test Specimen.

RESULTS AND DISCUSSIONS

• Visual Inspection

General and close-up views of cross sections of welded joints are shown in Fig. 4. No welding defects were detected. Figure 4 shows that the curves of cap pass for three specimens are smooth and good root penetration as well as smooth weld bead reinforcement morphology is obtained.

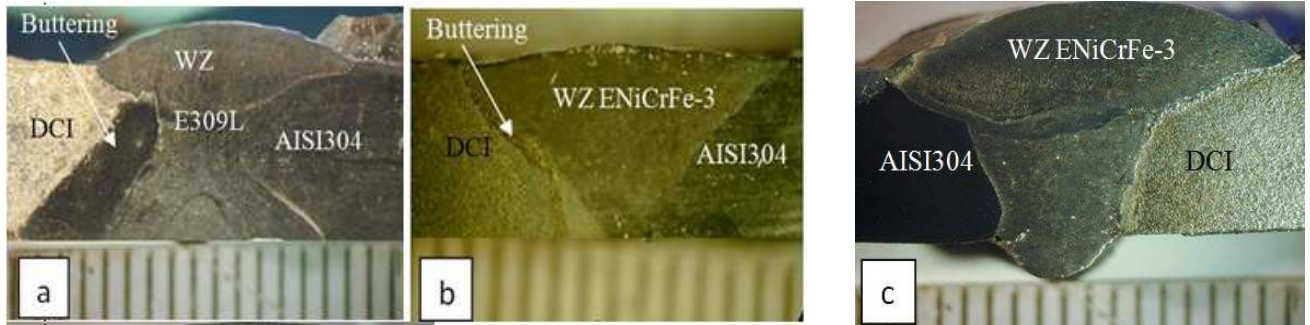


Figure 4: Cross Section at Dissimilar Welded Joints A) Buttering By Enife-CI and Filling E309L, B) Buttering by AL/Bronze and Filling by Enicrfe-3 & C) Without Buttering and Filling by Enicrfe-3.

• Microstructure of Dissimilar Welded Joints

Microstructure of dissimilar DCI/304 stainless sample 1 using buttering electrode (ENiFe-CI) at DCI side and complete filling the joint with E309L electrode is shown in Figs. 5 and 6. Microstructure of DCI base metal consists of coarse graphite nodules formed in ferrite matrix. By using (ENiFe-CI) electrode for buttering the DCI side, fine graphite nodules homogeneously distributed in the buttered layer. By using E309L welding electrode for V groove filling, no graphite nodules were formed in the weld zone (WZ). The buttering layer prevents further formation of graphite in weld zone; it also acts as an obstacle in carbon migration from DCI into weld zone to react with Cr to form chromium carbide. Weld zone microstructure contains a cellular grain formed at the interface growing toward the weld zone centre. This microstructure consists of austenitic matrix (white) with few ferrite phases (grey) formed in the matrix as shown in Figure 6.

Scanning electron microscopy (SEM) is used to investigate microstructure at high magnification of sample 1 the microstructure at DCI/buttering layer interface as shown in Figure 7 shows nodular graphite in matrix of DCI base metal and fine graphite nodules homogeneously distributed in the buttered layer as shown in Fig. 7a. In figure 7b show the mix of iron carbides at DCI/buttering interface which formed a result of melting and rapid cooling. The microstructure of weld zone show no graphite was detected as shown in Figure 7c.

Figure 8 shows EDX analysis of phases exist in HAZ of DCI for sample 1 together with their corresponding chemical composition are shown in Fig. 8, the elements existence at nodular graphite C-Si-Fe and elements existence in the grey matrix phase is C-Si-Fe are shown in Figure 8.

Results of EDX analysis of the buttering layer, weld zone and AISI304 phases are shown in Figure 9 the elements existence in buttering layer revealed elements of C-Si-Fe-Ni as shown in Fig. 9a, the elements existence in WZ matrix revealed elements C-Si-Cr-Fe-Ni are shown in Fig. 9b it also no visible graphite in weld zone was detected.

In case of sample 2 the ductile cast iron edge was buttered using Al-bronze filler (ER Cu Al- A2) and the dissimilar joint welded using ENiCrFe-3 electrode for filling V-groove. The microstructure of sample 2 weld joint at the DCI/WZ interface is shown in Fig. 10 Microstructure of ductile cast iron base metal consists of graphite nodules formed in

ferritic matrix. Compacted graphite and martensite in the buttered and HAZ zones are obvious. The weld zone (WZ) consists of lamellar grey and round white contrast phases formed in austenitic matrix. No visible graphite in WZ was detected.

SEM microstructures of sample 2 weld joint at the DCI/WZ interface are shown in Figure 11. Microstructure of ductile cast iron base metal consists of graphite nodules formed in ferritic matrix. Compacted graphite and martensite in the buttered and HAZ zones are obvious. The weld zone (WZ) consists of lamellar grey and round white contrast phases formed in austenitic matrix. No visible graphite in WZ was detected.

Results of EDX analysis of the weld zone phases are shown in Figure 12. EDX analysis of WZ matrix revealed existence elements of Ni-Fe-Cr-Mn-C. In addition, Cu-Al was detected in WZ due to dilution of the WZ with buttered layer of Cu-10Al filler. Al was detected in the buttered layer which might form Al-carbide, which highly expect to increase hardness in the buttered layer. It also obvious that Cr dissolved in WZ matrix are reduced to 10 wt.% from original content of filler metal composition (17 % Cr) content in filler metal due to formation of Cr- carbide (grey) and Nb-carbide precipitates (white) phase. EDX analysis of the white round phase in WZ reveals that this phase is Nb-carbide as shown in Figure 12c.

Heat affected zone of DCI revealed lamellar grey phase, with EDX analysis of these phase shows Si, Fe-carbides with composition as shown in Figs. 13a. This phase is formed due to a rapid cooling. In buttering layer the existence element revealed C-Al-Si-Cr-Fe-Ni-Cu-Nb which form Al, Nb, Cr, Fe- Carbides as shown in Fig. 13b.

Microstructure of sample 3 welded joint using ENiCrFe-3 electrode without buttering layer for V-groove passes are shown in Figure 14, Microstructures of DCI/WZ interface and stainless 304/WZ interface are shown in Figures 14 a & b respectively. At weld zone Cr-carbide as well as Nb and Ti carbides are formed in weld zone in austenitic matrix.

SEM microstructure of sample 3 shows the microstructure of ductile cast iron base metal consists of two phases with black contrast round phase (graphite) formed in ferritic matrix. Microstructure of weld zone reveals that microstructure mainly consists of three phases black contrast having irregular and round morphology and grey round phases formed in white phase matrix. On using ENiCrFe-3 for filling passes, no graphite was formed since carbon react with Cr, Nb and Ti to form Cr-carbide, (Nb, Ti) carbide instead of graphite formation, Figure 15. The microstructure at DCI/WZ interface reveals lamellar grey phase as shown in Figure 15.

EDX analysis of phases exist in sample joint 3 together with their chemical composition are shown in Figures 16 & 17. EDX analysis of the weld zone is white contrast phase is mainly (Nb) carbide precipitate as shown in Figure 16a. In addition, Fe-carbides in form lamellar grey at DCI/WZ interface as shown in Figure 16b. Obvious in weld zone no graphite was formed since carbon react with Cr, Nb and Ti to form Cr-carbide, (Nb, Ti) carbide instead of graphite formation as shown in Figures 17 (a, b, c). EDX analysis of phases at AISI304/WZ interface revealed existence elements C-Cr-Mn-Fe-Ni as shown in Figure 17d.

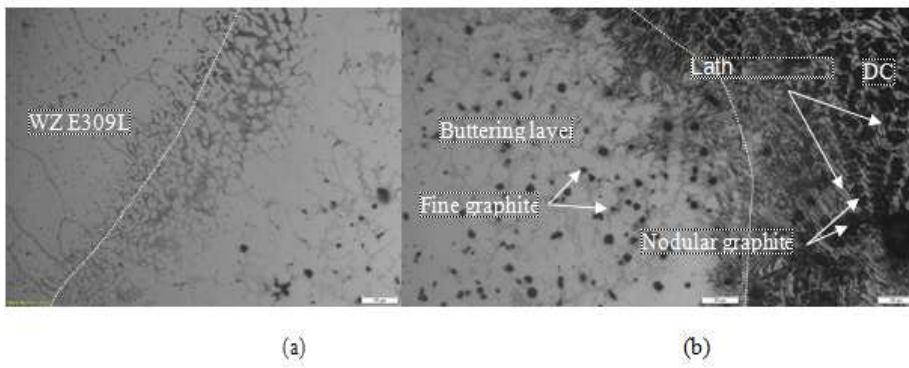


Fig. 5 Microstructure of Dissimilar DCI To AISI304 Welded Joint Using Enife-CI Electrode for Buttering DCI Side and Filling the Gap of the Joint Using E309L Electrode, the Interface At DCI/WZ.

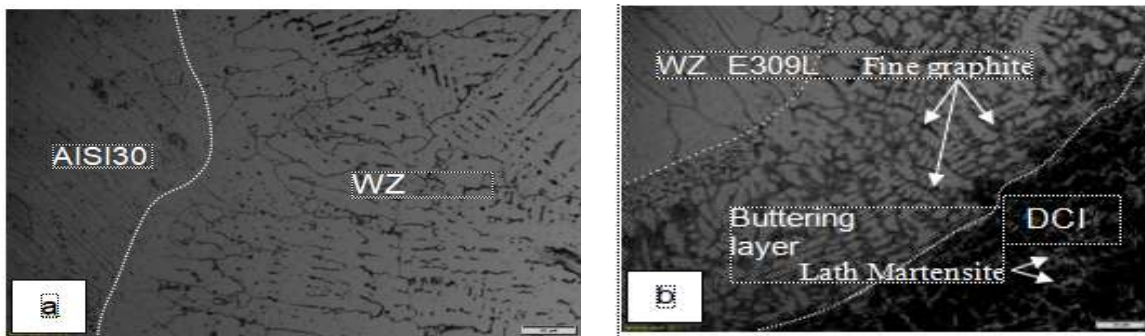


Figure 6: Microstructure of Dissimilar DCI to AISI304 Welded Joint Using Enife-CI Electrode For Buttering DCI Side and Filling The Gap of the Joint Using E309L Electrode, A) The Interface At AISI304/WZ, B) The Interface at DCI/WZ.

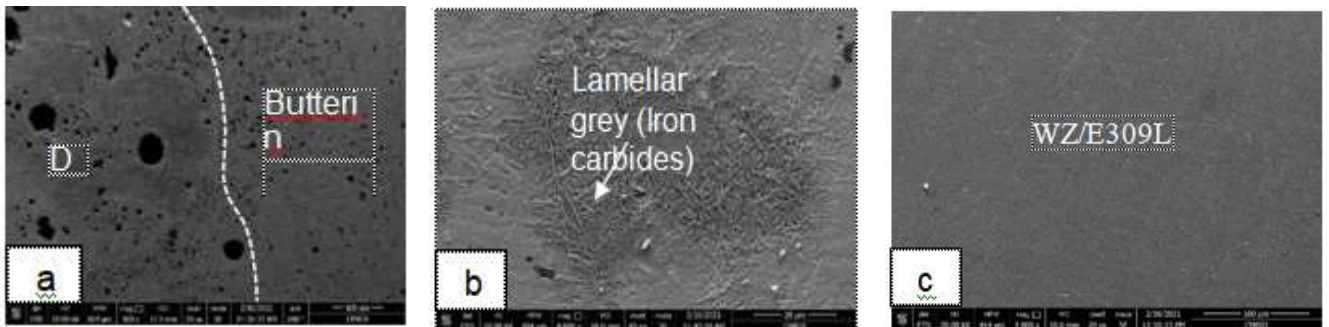


Figure 7: SEM Microstructure at DCI/Buttering Layer Interface, Weld Zone and Base AISI304.

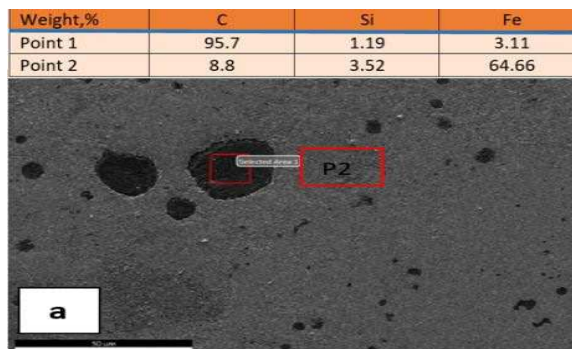


Figure 8: EDX Analysis of Phases Exists in HAZ of DCI For Sample 1.

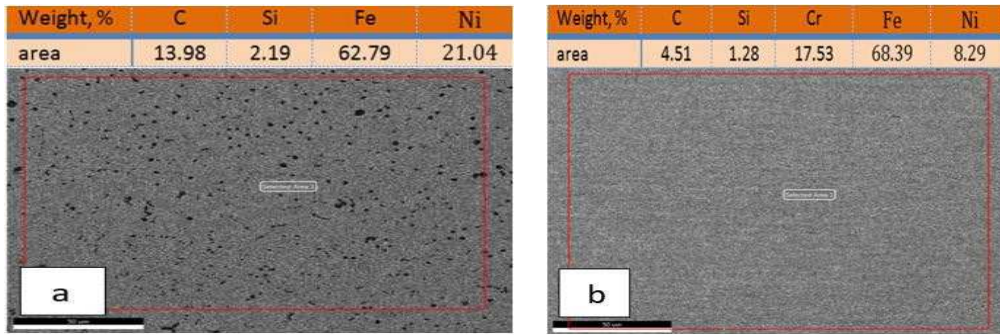


Figure 9: EDX Analysis of Sample 1 Weld Joint Using Enife-CI for Buttering and Complete Filling V-Groove Using E309L.

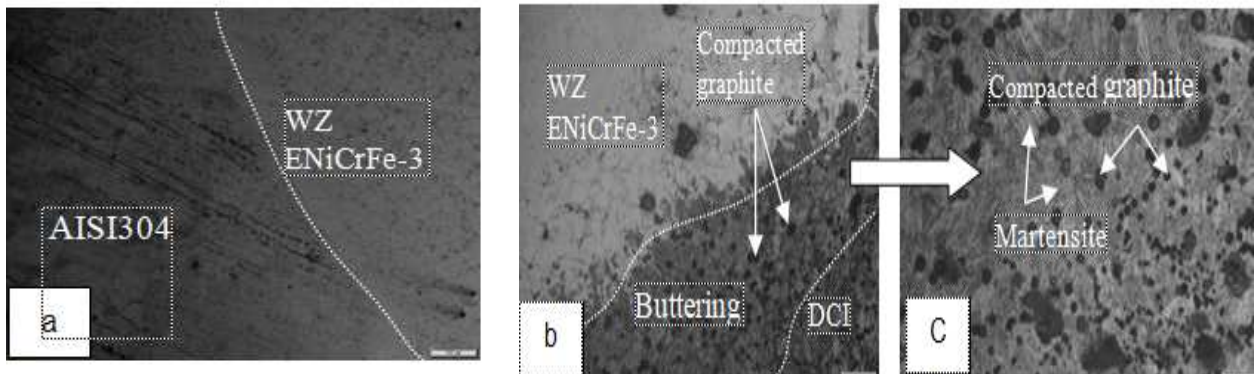


Figure 10: Microstructure of Dissimilar Welded Joint Using Al/Bronze for Buttering DCI Side and Filling the Gap of the Joint Using Enicrfe-3, a) The Interface at AISI304/WZ, b) the Interface at DCI/WZ, c) Magnification of Microstructure Buttering Layer.

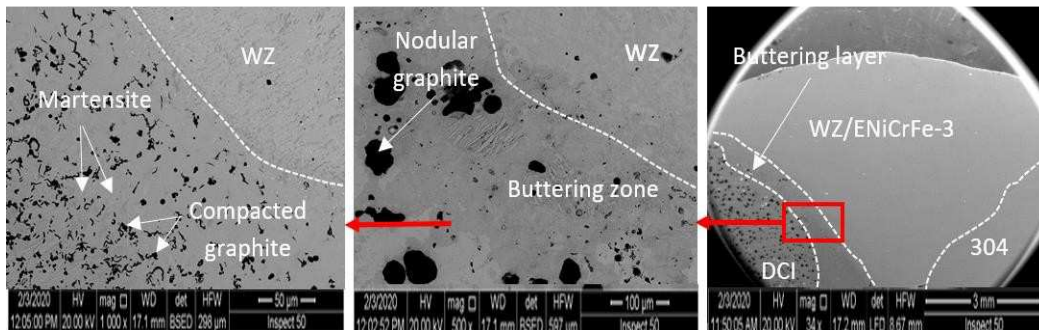


Figure 11: SEM Micrographs of Sample 2 Welded Joint at Ductile C.I/WZ Interface are Showing Microstructure of Ductile Cast Iron Base Having Graphite Nodules.

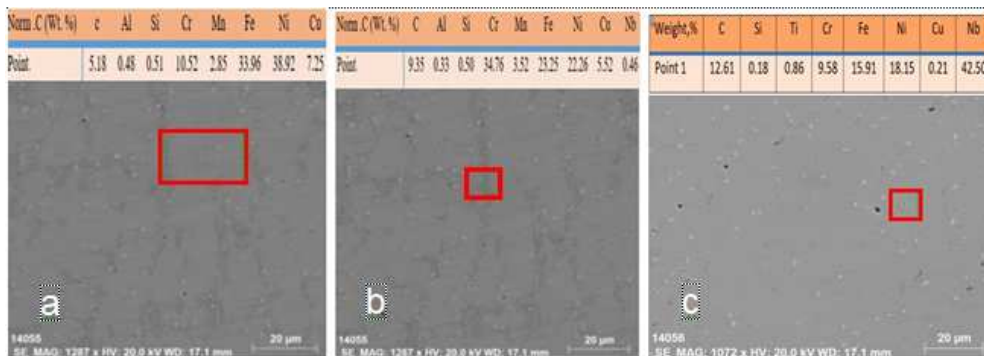


Figure 12: EDX Analysis of Weld Zone Matrix of Specimen 2.

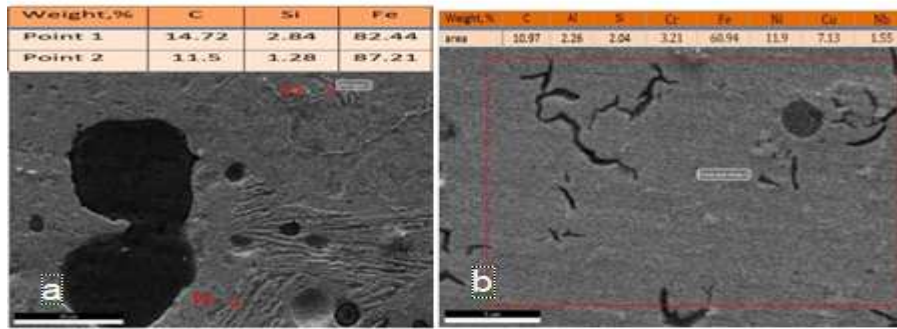


Figure 13: EDX of HAZ and Buttering Layer for Sample Joint 2.



Figure 14: Microstructures of Welded Joints by Electrode ENiCrFe-3, a) the Interface at DCI/WZ, b) the Interface at AISI304/WZ Side.

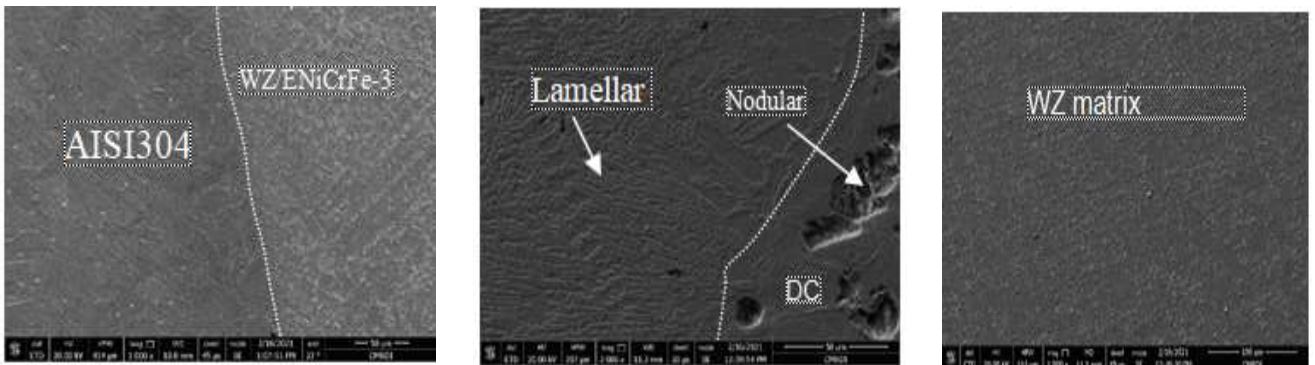


Figure 15: SEM Microstructure of Sample 3 Joint Welded Using ENiCrFe-3.

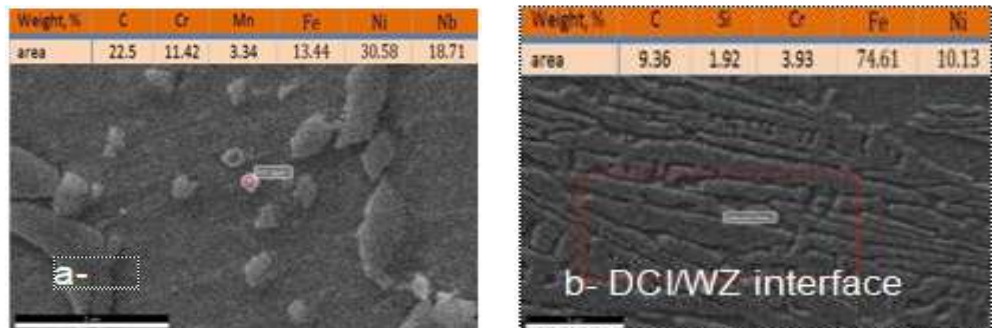


Figure 16: EDX of White Phase in Weld Zone and DCI/WZ of Specimen 3

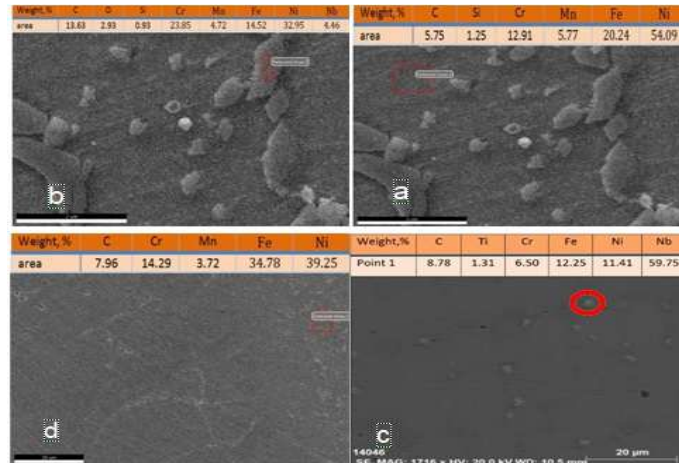


Figure 17: EDX of WZ and AISI304/WZ Interface of Specimen 3 Near DCI.

• **Mechanical Properties**

Microhardness Evaluation of Welded Joints

Figure 18 shows the hardness profiles of cross section dissimilar welded joints. In case of welding without buttering layer sample No. 3, the hardness value is increased gradually from DCI base metal to WZ due to diffusion of carbon from DCI side towards WZ then decrease gradually toward in WZ towards WZ/AISI 304 side. On using AL-bronze filler for buttering DCI side sample No. 2, the hardness increased at HAZ due to martensite formation. The increase in hardness at DCI/WZ interface is attributed to formation of aluminium carbide. Aluminium in filler metal reacts with carbon to form aluminium carbide thus hardness Drastically increased at fusion line is shown in Fig. 18 and gives hardness value of 720HV. However, existence of aluminium in the butter layer prevents carbon migration from DCI side to the weld zone and thus hardness is decrease. In sample No. 1 (buttering with ENiFe- CI and filling with E309L) the hardness values were the lowest compare with samples No. 2 and 3 and this may be attributed to the highest heat input for this welded sample and this leads to lowest rate of cooling and lowest hardness.

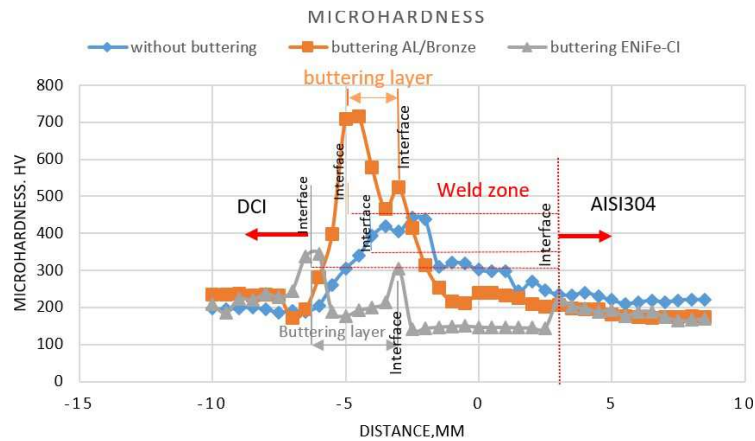


Figure 18: Hardness Profile for Dissimilar Welded Joints.

Tensile Test

Figure 19 shows the results of tensile test for welded specimens. In general, the results of tensile test are correspondent with the results of hardness test. All the samples were filed at the interface of DCI/buttering layer or DCI/WZ (in case of no buttering). The fracture surfaces of tensile test samples were investigated with SEM as shown in Figs. 20 and 21. Sample

No. 2 which buttering with ERCuAl-A2 and fill the joint with ENiCrFe-3 electrode has the highest tensile strength (TS) of 422MPa and fracture location was in partial fusion zone (PFZ) of DCI, SEM fractography of sample 2 reveal ductile fracture of weld zone (WZ) on using ENiCrFe-3 welding electrode while mixed ductile and brittle fracture of ductile cast iron, and no graphite can be seen in WZ as shown in Fig. 20. A crack is observed at ductile cast iron/weld zone interface due to the highest hardness value at this zone.

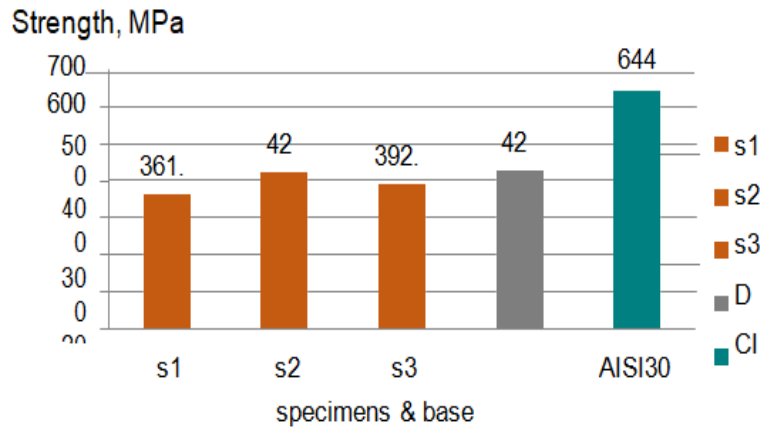


Figure 19: Tensile Strength of Welded Joints.

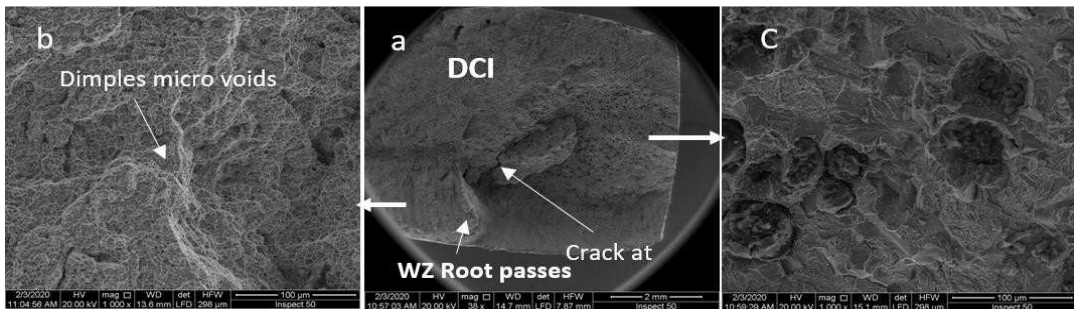


Figure 20: SEM Fractography of Tensile Tested Sample 2 Showing (A) General View of the Weld Joint Fracture Surface, (B) Ductile Fracture Weld Zone & (C) Mixed Ductile and Brittle Fracture of Ductile Iron, Cracks Are Visible At The Ductile Iron/Weld Zone Interface.

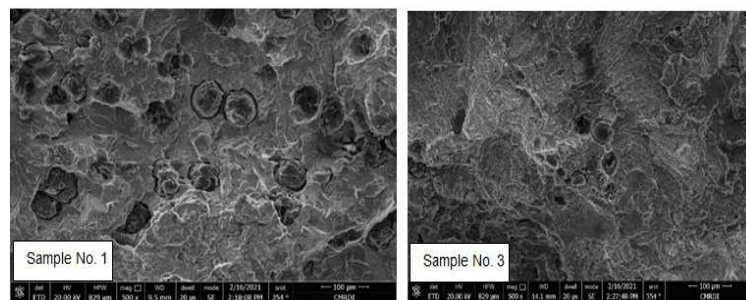


Figure 21: Fracture Surfaces of Samples 3 and 1, Respectively.

Impact Test

Impact test is carried out at room temperature on standard machined specimens taken from predetermined locations in HAZ of DCI while the other specimens taken in HAZ of AISI304 welded joints according to ASME code section IX. The impact values are so close to each other, the impact values at DCI side are lower compare to AISI304 side due to high concentrate of carbon content at HAZ near DCI as show in Figure 22.

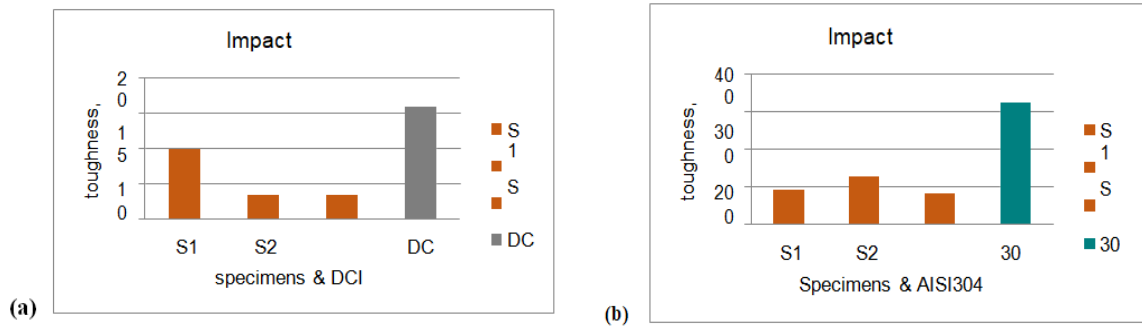


Figure 22: Impact Toughness of (a) HAZ of DCI Side and (b) HAZ of AISI304 Side.

CONCLUSIONS

In this study, dissimilar welding of ductile cast iron DCI grade A536 with austenitic stainless steel AISI304 using buttering with different? Or without buttering was investigated. Both microstructure and mechanical properties of welded joints are studied. The following conclusions can be concluded from this study as follows:

- The sample welded using buttering layer (ER Cu Al-A2) and filling groove with electrode ENiCrFe-3 has better mechanical properties compared with same sample without buttering technique.
- In general, when using buttering technique at DCI side it acts as obstacle layer to minimize carbon migration from DCI side to the weld and reduce formation of carbides in weld metal.
- Sample with buttering layer (ER Cu AL-A2) and welded with filler electrode (E NiCrFe3) has the higher strength hardness values compare with the sample which has buttering layer (E NiFeCI) and welded with filling electrode (E309L) has the lowest strength and hardness.
- The presence of elements such as Al, Ti, Cr and Nb in filler metals of both buttering layer (ER Cu Al-A2) and filling groove with electrode (ENiCrFe3) can increase the joint strength and hardness due to formation of carbides of these elements.
- Sample with buttering layer (ENiFeCI) and filling with (E309L) has higher impact toughness at HAZ of DCI side due to lower hardness of this sample as a result of high heat input during welding.

REFERENCES

1. <https://www.victaulic.com/blog/ductile-iron-coupling-for-stainless-steel-pipes>.
2. *Metals handbook the 9th Edition, volume 6, welding book, pp. (1749, 2045-2050).*
3. M. Hatate, *Bonding characteristics of spheroidal graphite cast iron and mild steel using electron beam welding process, Vacuum 73 (2004), pp. 667-671.*
4. Kamota S., Sakai M., Tagashira K., Igarashi M. and Akanuma M., *J Jpn. Inst. Met. (1988); 52:348–53.*
5. Yara H., Ikuta A. and Fujiki D., *J. Weld. Soc. Jpn. (1993); 11:474–80.*
6. Kamota S., Noguchi T., Sato T. and Sakai M., *J. Jpn. Foundrymen's Soc., (1992); 64:26– 32.*
7. Shibata F., *J. Jpn. Foundrymen's Soc., (1988); 60:666–72.*

8. Hiratsuka S., Nakamura M. and Horie H., *Jpn. Foundrymen's Soc.*, (1991); 63:589–95.
9. M. El-Shennawy, Adel A. Omar, *Similar and dissimilar welding of ductile cast iron, 6th matador conference.*
10. E. M. El-Banna, *Effect of preheat on welding of ductile cast iron, materials letters 41 (1999), pp. 20-26*
11. E. M. El-Bannaa, M. S. Nagedaa, M. M. Abo El-Saadab, *Study of restoration by welding of pearlitic ductile cast iron, Volume 42, Issue 5, February 2000, Pp. 311-320.*
12. D. W. Rathord, P. Singh, S. Pandey and S. Aravindan, *Effect of buffer-layered buttering on microstructure and mechanical properties of dissimilar metal weld joints for nuclear application, June 2016, Material Science and Engineering.*
13. S. Kolukisa, *The effect of the welding temperature on the weldability in diffusion welding of martensitic (AISI 420) stainless steel with ductile (spheroidal graphite – nodular) cast iron material processing technology 186 (2007), pp. 33-36.*
14. R. Winiuczenko and M. Kaczorowski, *Friction welding of ductile cast iron using interlayer, Materials and Design, 34 (2012), pp. 444-451.*
15. M. J. Houle and R. D. MC Guire, *CASTING Guide book to ASME section 9, Welding Qualifications, Third Edition.*

